Received: 26 August 2018 | Accepted: 4 October 2018

DOI: 10.1111/gcb.14543

PRIMARY RESEARCH ARTICLE

WILEY Global Change Biology

Fire deficits have increased drought sensitivity in dry conifer forests: Fire frequency and tree-ring carbon isotope evidence from Central Oregon

Steven L. Voelker[1] | Andrew G. Merschel[2] | Frederick C. Meinzer[3] | Danielle E. M. Ulrich[4] | Thomas A. Spies[5] | Christopher J. Still[2]

[1]Plants, Soils and Climate Department, Utah State University, Logan, Utah

[2]Department of Forest Ecosystems and Society, Oregon State University, Corvallis, Oregon

[3]Pacific Northwest Research Station, USDA Forest Service, Corvallis, Oregon

[4]Los Alamos National Laboratory, Los Alamos, New Mexico

[5]USDA Forest Service Pacific Northwest Research Station, Portland, Oregon

Correspondence
Steven L. Voelker, Plants, Soils and Climate Department, Utah State University, Logan, UT.
Email: dr.s.voelker@gmail.com

Funding information
USDA Forest Service, Grant/Award Number: Joint venture agreement 14-JV-1126191952-095; Oregon State University; Utah Agricultural Experiment Station Project 1304

Abstract

A century of fire suppression across the Western United States has led to more crowded forests and increased competition for resources. Studies of forest thinning or stand conditions after mortality events have provided indirect evidence for how competition can promote drought stress and predispose forests to severe fire and/or bark beetle outbreaks. Here, we demonstrate linkages between fire deficits and increasing drought stress through analyses of annually resolved tree-ring growth, fire scars, and carbon isotope discrimination ($\Delta^{13}C$) across a dry mixed-conifer forest landscape. Fire deficits across the study area have increased the sensitivity of leaf gas exchange to drought stress over the past >100 years. Since 1910, stand basal area in these forests has more than doubled and fire-return intervals have increased from 25 to 140 years. Meanwhile, the portion of interannual variation in tree-ring $\Delta^{13}C$ explained by the Palmer Drought Severity Index has more than doubled in *ca*. 300–500-year-old *Pinus ponderosa* as well as in fire-intolerant, *ca*. 90–190-year-old *Abies grandis*. Drought stress has increased in stands with a basal area of ≥25 m^2/ha in 1910, as indicated by negative temporal $\Delta^{13}C$ trends, whereas stands with basal area ≤25 m^2/ha in 1910, due to frequent or intense wildfire activity in decades beforehand, were initially buffered from increased drought stress and have benefited more from rising ambient carbon dioxide concentrations, [CO_2], as demonstrated by positive temporal $\Delta^{13}C$ trends. Furthermore, the average $\Delta^{13}C$ response across all *P. ponderosa* since 1830 indicates that photosynthetic assimilation rates and stomatal conductance have been reduced by ~10% and ~20%, respectively, compared to expected trends due to increasing [CO_2]. Although disturbance legacies contribute to local-scale intensity of drought stress, fire deficits have reduced drought resistance of mixed-conifer forests and made them more susceptible to challenges by pests and pathogens and other disturbances.

KEYWORDS
basal area, carbon isotope discrimination, CO_2, drought resistance, fire suppression, ponderosa pine, stand density, stomatal conductance

1 | INTRODUCTION

The structure and functioning of dry montane forest landscapes of the Western United States were historically maintained by frequent low- to mixed-severity fire regimes, but have experienced widespread fire deficits since a federal policy of fire suppression was enacted in 1910 (Bekker & Taylor, 2001; Parks et al., 2015; Pyne, 1982; Smith & Arno, 1999). In combination with grazing, logging, and land-use changes, fire suppression has caused productive older forests of this type to undergo radical changes in their structure as shade-tolerant and fire-intolerant species have established and filled in gaps and mid-story canopy positions (Covington & Moore, 1994; Hagmann, Franklin, & Johnson, 2013, 2014; Hessburg et al., 2016; Johnston, 2017; Merschel, Spies, & Heyerdahl, 2014; Smith & Arno, 1999). During the same period, atmospheric carbon dioxide concentrations, [CO_2], have been rising at increasing rates, modifying leaf gas exchange (Voelker et al., 2016). Although increasing [CO_2] and succession after fire suppression are both expected to strongly influence forest function, their collective importance for resistance to drought and associated forest landscape resilience over the past >100 years has not previously been documented in detail.

There is an emerging realization that forested landscapes have been increasing in stand density and basal area with cascading ecological effects (Spies, Hessburg, & Skinner, 2018). These widespread changes across the Western United States have prompted concern about an ongoing erosion of resistance to drought and resilience to insect and disease outbreaks, and wildfires (Hessburg et al., 2016; Johnstone et al., 2016). For this study, we define resistance to drought in terms of the impact of drought on stomatal conductance and net carbon gain under a given set of meteorological conditions. Hence, for a given level of precipitation and evaporative demand, trees undergoing more belowground competition for water will have lower drought resistance, or conversely, be more sensitive to drought. This is similar to how resistance has been defined when referring to tree growth responses to drought (Bottero et al., 2017; Lloret, Keeling, & Sala, 2011). In turn, lowered resistance to drought often increases susceptibility to insect attacks and outbreaks (Anderegg et al., 2015; Raffa et al., 2008). Here, we use the term resilience to describe the degree to which forests, at a landscape scale, may be able to retain or recover their ecosystem functions when challenged by disturbances such as fire and insect outbreaks that are often linked to drought stress.

More crowded forests with abundant understory and mid-story trees have greater vertical and horizontal fuel connectivity that can promote increased fire spread and more and/or larger patches of high-severity fire, depending on forest canopy connectivity, compared to more open historical conditions (Kalies & Yocom Kent, 2016; Safford, Schmidt, & Carlson, 2009; Stephens, 1998). The risk of fire is not independent of other concerns for forest health. Forests with greater stand occupancy (i.e., greater tree density for a given average tree size) tend to suffer greater mortality rates during and after significant droughts, particularly in association with pests and pathogen attacks (Bottero et al., 2017; Bradford & Bell, 2017; Fettig et al., 2007; Fettig, Mortenson, Bulaon, & Foulk, 2019; Voelker, Muzika, & Guyette, 2008; Young et al., 2017). Furthermore, fire exclusion can increase the risk of bark beetle-related tree mortality compared to forests that have been exposed to repeated low-severity fires that increase tree defenses against bark beetle attacks (Hood, Baker, & Sala, 2016; Hood, Sala, Heyerdahl, & Boutin, 2015). Finally, prolonged drought stress prior to a surface fire, as is more likely to occur under crowded forest conditions, results in surviving trees being more likely to die in subsequent years after fires, independent of fire intensity (van Mantgem et al., 2013). These studies document the generality of how stand density and basal area exceeding a certain threshold (sensu Jump et al., 2017) can interact with drought and fire deficits (sensu Parks et al., 2015) to predispose forests to large-scale mortality events such as the ongoing pulse of mortality of at least 102 million trees across 7.7 million acres in California during 2010–2016 (Moore, McAfee, Jirka, Heath, & Smith, 2017). The widespread nature of fire exclusion across dry mixed-conifer forests of the Western United States suggests a landscape scale loss of resistance to natural disturbance processes as well as a loss of resilience after droughts, fires, or insect outbreaks inevitably occur.

Determining the mechanistic underpinnings of how greater stand occupancy leads to increased drought stress has proven to be elusive. Toward this end, a biophysical modeling approach has been used to estimate changes in drought stress due to stand occupancy and climate (Lutz, Wagtendonk, & Franklin, 2010). The effects of stand occupancy have also been demonstrated in reverse, where forest thinning has relieved drought stress and made stands more resistant to some beetle outbreaks (Bottero et al., 2017; Dore et al., 2012; Giuggiola et al., 2016; Hood et al., 2016; McDowell, Adams, Bailey, Hess, & Kolb, 2006; McDowell, Brooks, Fitzgerald, & Bond, 2003; Sohn, Saha, & Bauhaus, 2016; Vernon, Sherriff, Mantgem, & Kane, 2018; Waring & Pitman, 1985). Although previous studies have provided key insights on tree responses to stand occupancy, competition, and climate, there is a lack of direct evidence documenting the extent to which drought stress has tracked fire deficits following fire suppression efforts starting in the early 20th century.

Tree-ring carbon isotope records from dry Western US forests have historically demonstrated a wide range of responses of intrinsic water use efficiency (iWUE) to rising [CO_2] since the first effort to summarize such trends by Feng (1998). Despite many subsequent studies, records with interannual resolution sampled over too short of a period or were aimed at addressing the impact of thinning treatments that reduced stand occupancy (Leavitt, Wright, & Long, 2002; Marshall & Monserud, 1996; McDowell et al., 2006; McDowell, Allen, & Marshall, 2010; Roden & Ehleringer, 2007; Sohn et al., 2014). Alternatively, other tree-ring carbon isotope studies of Western US forests used pentadal or decadal sampling units that preclude determinations of sensitivity to meteorological drought on a year-by-year basis (Feng, 1998; Knapp & Soulé, 2011; Knapp, Soulé, & Maxwell, 2013; Leavitt & Long, 1988; Reed, Ballantyne, Cooper, & Sala, 2018; Soulé & Knapp, 2015). Additional ponderosa pine tree-ring carbon isotope records with interannual resolution have been

developed but offer no insight on responses to competition since the sites chosen had widely spaced trees to help ensure the stability of climate responses (Szejner et al., 2016; Szejner et al., 2018).

Despite the numerous tree-ring carbon isotope studies from dry forest sites spanning much of the Western United States, it is unclear whether rising [CO_2] concentrations and increasing iWUE may have ameliorated drought stress induced by increased stand occupancy, or whether successional and structural changes have caused forests to become more sensitive to drought despite rising [CO_2]. Here, we examine these questions in detail at a site in Central Oregon where fire history has been studied intensively (Figure 1; Merschel, Heyerdahl, & Spies, 2018). We use forest inventory methods paired with tree growth and age data from increment cores, an extensive multicentury record of historical surface fires, and annually resolved tree-ring carbon isotope records from individual old ponderosa pine and younger, relatively fire- and drought-intolerant grand fir trees. The overarching goals of this study are to document the trajectory of sensitivity to drought stress in response to progressively increasing fire deficits and the threshold level of stand occupancy which conveys decreasing resistance and resilience to drought stress, bark beetles, and wildfire.

2 | MATERIALS AND METHODS

2.1 | Characterization of the study area

Merschel et al. (2018) characterized topography, forest composition and structure, and the historical pattern of fire in detail across a 10,000 ha area that encompasses our >2,800 ha study area southwest of Bend, Oregon (Figures 1a1–7d). Elevation change is gradual besides the volcanic cinder cones and flat pumice basins that do not strongly factor into the sampling of this study (Figure 1a). The range in annual precipitation of approximately 60–110 cm and mean annual maximum temperature of 11–14°C across the study site was captured by fire history and tree-ring stable isotope sampling (Figures 1b1–7c). At the lowest elevations of the study area (1,350 m), the forest composition is nearly pure ponderosa pine, whereas less fire-tolerant species such as grand fir, western white pine (*Pinus monticola*), and mountain hemlock (*Tsuga mertensiana*) are increasingly present at elevations nearing or above 1,850 m. Lodgepole pine (*Pinus contorta*) forms nearly pure stands in flat basins with pumice soils but also occurred as a minor component in some of the stands sampled for this study. A portion of the study area was heavily logged between 1920 and 1940, but trees identified for stable isotope analyses were not sampled from these areas.

2.2 | Forest inventory and tree-ring sampling

Sampling procedures are detailed in Merschel et al. (2018), but we summarize the methods here. We established 28 sample plots systematically using a grid with 1 km spacing to characterize current and historical forest structure and composition and reconstruct fire history (Figure 1a). Where plot locations were initially located in areas with past intensive management or near a road, plot locations were moved to the nearest area with intact old-growth forest.

To characterize structure and composition and tree demography at each plot, we established variable radius plots for three tree size classes: small: 5–29 cm diameter at a breast height of 1.4 m (DBH), medium: 30–49 cm DBH, and large: >50 cm DBH. Small trees were also tallied within a 7.28 m radius plot. Where possible we selected the nearest 12 medium and 12 large trees per plot and recorded their species, DBH, and status (i.e., live, log, snag, or stump). If fewer than 12 such trees occurred within 28.2 and 40.0 m of plot center, respectively, we selected additional medium and then small trees within the same distances until 24 total trees were characterized. From these 24 trees, we removed 5-mm-diameter increment cores at a stem height of 40 cm. From dead trees, we removed partial cross sections at 40 cm with a chain saw, including the pith where possible. For trees lacking intact wood, we recorded species and diameter, then sampled a proxy tree of the same species, status, and similar diameter within 100 m.

To reconstruct fire history, we searched for fire-scarred trees within 250 m of each plot center and removed partial cross sections (Arno & Sneck, 1977) from 3–8 trees per plot. Three plots lacked

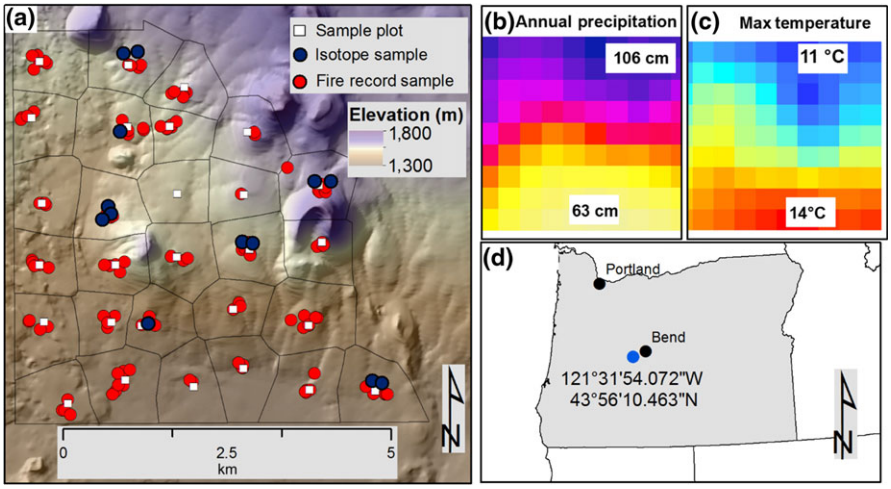

FIGURE 1 Study area showing the locations of sampled fire-scarred trees within fire history reconstruction polygons (after Merschel et al., 2018), and trees sampled for carbon stable isotopes (a). Variation in precipitation (b) and temperature (c) across the study area. Location of the study area, southwest of Bend, Oregon, USA, is highlighted in blue (d) [Colour figure can be viewed at wileyonlinelibrary.com]

trees with fire scars prior to 1870. Two of these plots were dominated by short-lived lodgepole pine; the third was a plot located in mixed-conifer forest that burned severely enough in 1868 that evidence of past fires was destroyed. Fire records during 1650–1910 were available at the remaining 25 plots.

2.3 | Dendrochronological methods

Increment cores and cross sections were surfaced with progressively finer sandpaper until cell structure was visible under a binocular microscope. Calendar years were assigned to annual rings using visual cross-dating. Thereafter, rings were measured using a sliding stage linear encoder (Velmex Inc., Bloomfield, NY, USA) and MeasureJ2X software (Voortech Consulting, Holderness, NH, USA) and verified using COFECHA software (Holmes, 1983). Tree cores and cross sections that did not cross-date (2%) were excluded from further analysis. For samples that did not intersect the pith, we estimated the number of rings to pith (sensu Applequist, 1958) unless it was estimated that the distance included >20 rings, in which case these samples were also excluded (<5% of samples). The calendar year in which of surface fires occurred was recorded, as detailed in Merschel et al. (2018), on partial cross sections from 122 trees.

2.4 | Tree-ring isotope sampling and analyses

We selected eight ponderosa pine trees and five grand fir trees for stable isotope sampling that represented a range of climate conditions (Figures 1a1–7c) in the southwest corner of the Merschel et al. (2018) fire regime reconstruction area because it had relatively intact old-growth stands. All wood from ponderosa pines and some grand firs came from wedges cut using a chainsaw. This provided one radius, but the width of that radius encompassed 3–6 cm, depending on the width of the rings. Wood from some grand firs was from three 12-mm-diameter increment cores. In all cases, the latewood of each tree was excised for stable isotope analyses. Only latewood was used because this portion of the annual ring generally forms during mid- to late summer, a period which should ostensibly capture interannual variation in drought stress more readily compared to whole-ring analyses. Indeed, studies from nearby locations on the west and east slopes of the Oregon Cascade Mountains have demonstrated that latewood carbon stable isotope signals strongly record summer drought conditions regardless of what tree species are chosen and across a range of annual precipitation of 350–2,500 mm (Ratcliff, Voelker, & Nolin, 2018; Roden & Ehleringer, 2007).

We used a Dremel brand (Robert Bosch Tool Company, Gerlingen, Germany) rotary tool to grind large rings (>0.5 mm), whereas small rings (<0.5 mm) were excised with a scalpel under a binocular microscope and ground to a fine powder using a Fisher Scientific PowerGen Homogenizer. Wood powder was heat-sealed within polyester/polyethylene-fiber filter bags (ANKOM, Fairport, NY) and purified to holocellulose following Leavitt and Danzer (1993). Holocellulose was weighed into tin capsules on a microbalance for analyses of carbon isotope composition, which is expressed relative to that of a standard using "delta" notation as $\delta^{13}C = (R_{sample}/R_{standard} - 1) \times 1{,}000$, where $\delta^{13}C$ is the molar ratio of heavy to light isotopes and $R_{standard}$ is Pee Dee Belemnite (PDB). $\delta^{13}C$ of each sample was obtained using standard high-temperature combustion in a vario-Pyrocube elemental analyzer interfaced with IsoPrime/Elementar IsoPrime 100 gas-phase isotope ratio mass spectrometer (IsoPrime Ltd., Manchester, UK) at the Roden Stable Isotope Laboratory at Southern Oregon University. The long-term precision does not exceed ±0.1 ‰ for $\delta^{13}C$ analyses at this facility. $\delta^{13}C$ data were converted to $\Delta^{13}C$ following Farquhar, Ehleringer, and Hubick (1989) as: $\Delta^{13}C = (\delta^{13}C_{air} - \delta^{13}C_{plant})/(1 + \delta^{13}C_{plant}/1{,}000)$ where $\delta^{13}C_{air}$ was estimated from McCarroll and Loader (2004) merged with more recent, annually averaged $\delta^{13}C_{air}$ records from Mauna Loa, Hawaii (http://scripps co2.ucsd.edu/data/atmospheric_co2/mlo)

2.5 | Comparisons of observed and predicted leaf gas exchange trajectories

Following Farquhar et al. (1989), cellulose $\Delta^{13}C$ data can be converted to ratios of leaf internal to ambient $[CO_2]$ (i.e., c_i/c_a) as follows:

$$c_i/c_a = (\Delta^{13}C - 4.4‰) / (27‰ - 4.4‰), \quad (1)$$

where 4.4‰ and 27‰ are fractionations related to molecular diffusion through stomatal pores and carboxylation by the Rubisco enzyme, respectively. To estimate how individual components of leaf gas exchange of ponderosa pines have been affected over the past 180 years by climate, $[CO_2]$ and increasing stand occupancy, we combined $\Delta^{13}C$ data with a species-specific A-c_i curve, which characterizes how photosynthetic assimilation rates (A) respond to the leaf internal $[CO_2]$ (c_i), as modified by changes in c_a and/or stomatal conductance (g_s). Following Ehleringer (1993), it can be shown that the intrinsic water use efficiency (iWUE), is proportional to the ratio of A/g_s as follows:

$$A/g_s = (c_a - c_i) / 1.6, \quad (2)$$

where 1.6 is the ratio of molecular diffusivities of water vapor and CO_2 in air. The empirically defined A-c_i curve employed in this research ($R^2 = 0.89$, $p < 0.0001$, *data not shown*) included 130 data points from six mature ponderosa pine trees located about 60 km to the North of the study location at the Metolius River Research Natural Area, which receives about 57 cm of precipitation annually. This relationship was defined as:

$$A = 9.8543 \times \ln(c_i) - 41.769. \quad (3)$$

To obtain leaf gas exchange estimates, we first estimated c_i for each year in the past by rearranging Equation 1 to solve for c_i and then inserting the observed $\Delta^{13}C$ mean for each year across all trees and values of c_a estimated from McCarroll and Loader (2004) merged with the Mauna Loa record as described above for records of $\delta^{13}C_{air}$. Thereafter, we inserted estimated c_i values into Equation 3 to solve for A for each year. Finally, to calculate g_s for each year

we rearranged Equation 2 for iWUE as $g_s = (1.6A)/(c_a - c_i)$ and inserted estimates noted above for A, c_a, and c_i. Finally, we compared interannual variation in A and g_s to the values expected from a global meta-analysis of how woody plants regulate leaf gas exchange in response to changes in c_a (Voelker et al., 2016). More specifically, we extracted the following relationship from Voelker et al. (2016) for the expected total change in c_i/c_a from the full glacial c_a minima of 190 ppm (i.e., $\Delta c_i/c_a$) as:

$$\Delta c_i/ca = -0.3974 + 0.5163 \times \left(1 - e^{(-0.0067 * ca)}\right). \quad (4)$$

First-order differences were calculated from Equation 4 and added to the average c_i/c_a value of ponderosa pine across the years 1830–1834. Thereafter, these values were converted to predicted changes in A and g_s using the same approach described above.

2.6 | Data preparation and statistical analyses

Interannual $\Delta^{13}C$ data compared to climate data were detrended with a 100-year cubic spline using ARSTAN software (Cook and Krusik 2014) to remove long-term trends owing to stand dynamics. Running correlations as well as linear regression models were constructed using the Treeclim (Zang & Biondi, 2015) or "lm" packages, respectively, in the R statistical computing environment (R Core Team, 2017). These were compared to reconstructed Palmer Drought Severity Index (PDSI) data previous to 2004 (Cook et al., 2010), which was then merged with instrumental Oregon Division 5 PDSI values for 2005–2014.

Pandora moth (*Coloradia pandora*) outbreaks are known to have defoliated ponderosa pines in this region (Speer, Swetnam, Wickman, & Youngblood, 2001). We inferred specific years for outbreaks after the methods of Speer et al. (2001). This included visual identification in tree cores, paired with tree-ring chronology data that confirmed suppression of growth of whole-ring and latewood specific data, especially when reconstructed PDSI values suggested these would otherwise be relatively wet or only moderately dry years. These methods identified four periods of defoliation occurred at our site which closely corresponded to the timeframes of regional defoliations inferred by Speer et al. (2001). We then determined whether defoliation affected sensitivity of interannual $\Delta^{13}C$ data to the reconstructed PDSI. We did so by using paired two-tailed t tests to compare the R^2 values between $\Delta^{13}C$ and PDSI averaged across the 10 year previous to each defoliation to the R^2 values averaged across (a) defoliation years only, (b) defoliation years and five subsequent years, and (c) defoliation years and 10 subsequent years. Given that there were only four defoliations to compare, these methods should only detect significant differences if there were strong changes in the sensitivity of $\Delta^{13}C$ to PDSI.

To reconstruct stand basal area in 1910, cross-dated basal area increments were subtracted from DBH measurements of live trees and the subsequent individual tree basal areas that remained were summed and divided by the plot area. Leaf area index (LAI) in 1910 was reconstructed based on basal area data, using the relationship between a 12-stand chronosequence of LAI and basal area presented in Law et al. (2003) for ponderosa pine stands from Central Oregon (LAI = 0.7577 ln(basal area)–0.9142, $R^2 = 0.72$, $p < 0.001$, *data not shown*). Results were visualized using SigmaPlot (Systat Software, Inc., San Jose, CA, USA).

3 | RESULTS

Fire reconstructions within 28 stands (i.e., polygons) across our study site indicated that the most common end date for fires was 1910, but two stands had not had a fire since 1887 or 1871 (Figure 2a). No evidence of fire was recorded at any stand from 1911 to 2015. During 1600–1910, there were 27 years when fire was recorded at >5 stands or across at least 500 ha, and 11 years when fire was recorded at ≥15 stands (e.g., more than half the sampled area (Figure 2b). The mean composite fire-return interval prior to 1910 ranged from 17 to 31 years among stands (Table 1). As expected, the stands selected for isotope sampling had a positive but weak relationship between historic fire-return interval before 1910 and stand basal area in 1910 (Table 1), reflecting the consistency in which fires were historically more frequent across this forested landscape but with diverse effects on the resulting forest structure as is typical in forests dominated by low- to mixed-severity fire regimes.

The extent of large fires cannot be determined since such fires surpassed the boundary of the sampling grid. Most of the ponderosa pines at the site were 150–400 years old, whereas most grand firs were <150 years old, with the greatest proportion being <100 years old (Figure 2c). We sampled trees for isotopic composition from seven stands varying in basal area and species composition, with five of seven stands increasing in basal area between 1910 and 2015 (Figure 2d). One exception was stand KC19, where basal area was high and did not change very much. In this stand, a dense understory of ponderosa pine replaced basal area previously occupied by large diameter ponderosa pine that were selectively cut or died during the 20th century. The other exception, stand KB16, had lower basal area due to logging in the late 1980s that removed most of the large ponderosa pines from that stand. Three of the seven stands showed substantial increases in basal area of grand fir presumably a result of fire exclusion. Correlations between $\Delta^{13}C$ and monthly meteorological variables indicate that PDSI was consistently important for determining interannual variation in leaf gas exchange of both ponderosa pine and grand fir (Table 2), reflecting both the importance of soil moisture as well as the highly correlated nature of the monthly calculation of PDSI. At this site, the relative influence of current year meteorological variables since 1950 did not differ sharply among variables associated with water supply or demand or between species, despite differing life history characteristics of ponderosa pine versus grand fir (Table 2). These data suggest that the historical distribution of grand fir for this region was determined more by susceptibility to damage or mortality by frequent fires than by drought stress. A closer examination of $\Delta^{13}C$ versus PDSI over time, using moving correlations shows that responses of leaf gas exchange to current year drought stress have been relatively stable for ponderosa

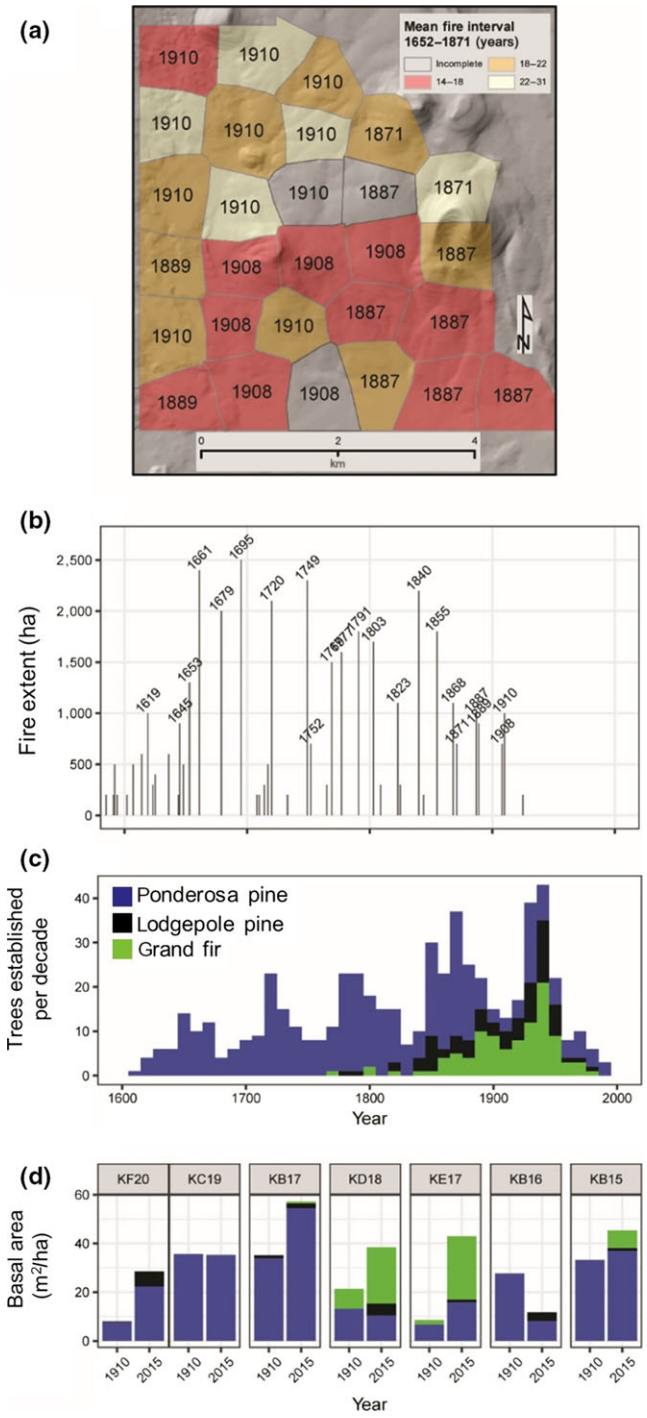

FIGURE 2 Aspects of fire history and tree establishment. The date of the last fire recorded in each fire reconstruction polygon (a), extent and timing of fires historically recorded by tree-ring fire scars (b), tree establishment by species (c), comparisons of basal area reconstructed for 1910 and that recently measured in 2015 for the seven stands where trees were sampled for tree-ring carbon isotopes (d). Years indicated on x-axis of panel (c) also applies to panel (b) [Colour figure can be viewed at wileyonlinelibrary.com]

pine since the early 1900s, whereas for grand fir, the responses increased from 1920 through 1980 before leveling off (Figure 3a). In ponderosa pine, the $\Delta^{13}C$ response to antecedent year PDSI exhibited a large trough from *ca.* 1910–1940 but then rose to the highest levels on record beginning *ca.* 1960 (Figure 3a). In contrast to the importance of antecedent year PDSI for ponderosa pine, this variable did not explain a significant amount of the variation in leaf gas exchange in any years for grand fir. By considering both current and antecedent year PDSI within a moving-window multiple regression model framework, the amount of variation explained increased by two- to threefold, tracking the trajectory of increasing average fire-return intervals (i.e., the absence of fire since 1910) across our study site (Figure 3b). Indeed, the amount of $\Delta^{13}C$ variation predicted by PDSI was strongly and nonlinearly related to fire-return interval, whereby fire-return intervals between 20 and 100 years strongly affected the sensitivity of leaf gas exchange to PDSI but had only weak effects as the length of fire-free intervals increased (Figure 4a). A comparison among species indicated the slope of $\Delta^{13}C$ predicted by log-transformed fire-return intervals (Figure 4b) for grand fir (R^2 = 0.54 log [FRI] − 0.55) was significantly steeper ($p < 0.001$) compared to the slope for ponderosa pine (R^2 = 0.33 log [FRI] − 0.20).

The above evidence linking variation in $\Delta^{13}C$ explained by PDSI to fire-return interval suggests that in most stands of mature ponderosa pine, trees are likely to be exposed to strong increases in competition for soil water any time fire-return intervals increase. However, we know that there was a large of degree of variation in stand occupancy near when fire suppression started in 1910 and that which has recently characterized these stands in 2015 (Figure 2d).

Another way of investigating drought stress in individual trees is to examine temporal trends in $\Delta^{13}C$ (Supporting Information Figure S1). For this site, a positive temporal trend in $\Delta^{13}C$ would suggest decreasing stomatal constraints on leaf gas exchange, whereas a negative temporal trend would suggest greater stomatal closure and drought stress. We calculated the slopes of trajectories of $\Delta^{13}C$ calculated since 1860 (Supporting Information Figure S1) for individual trees. This period was chosen because it allows a nearly full representation of $\Delta^{13}C$ data available for ponderosa pine trees while also allowing for the inclusion of data from the two oldest grand firs sampled. These trends plotted versus stand-level basal area in 2015 showed no significant pattern (R^2 = 0.18, p = 0.22; Figure 5a). The same response variable plotted versus the reconstructed stand-level basal area or leaf area index in 1910 displayed a strong negative linear relationships ($R^2 \geq 0.83$, $p < 0.001$; Figure 5b,c). Hence, stand basal area and leaf area conditions in 1910, at the start of the fire suppression era, had a strong role in determining whether a tree became increasingly drought-stressed or not over the subsequent 105 years.

Temporal trends in $\Delta^{13}C$ can also be used to identify which trees may be more sensitive to climatic stress and therefore more suitable for identifying which climate variables are most responsible for driving increased drought stress. Toward this end, we plotted the slopes of the temporal trends in $\Delta^{13}C$ for individual trees (see Supporting Information Figure S1 for example) versus the correlations between detrended $\Delta^{13}C$ and summer maximum temperatures, summer vapor

TABLE 1 Tree and stand characteristics at the study area in Central Oregon

Tree or stand property	*Pinus ponderosa*								*Abies grandis*				
Tree number	1	2	3	4	10	11	12	13	5	6	7	8	9
Pith date year*	1724	1634*	1514*	1690*	1575	1772	1718	1769	1885	1825	1825	1925	1932
DBH (cm)	81	161	95	110	112	74	84	96	65	96	101	76	71
Stand identification	KB16	KB15	KB15	KB17	KE17	KF20	KC19	KF20	KE17	KD18	KD18	KB17	KB17
Year of last fire	1910	1910	1910	1910	1871	1887	1910	1887	1871	1908	1908	1910	1910
Historic fire-return interval (years)	19	31	31	24	24	17	18	17	24	18	18	24	24
Total basal area in 1910 (m^2/ha)	27.7	33.3	33.3	35.2	8.5	8.1	35.7	8.1	8.5	21.4	21.4	35.2	35.2
Total basal area in 2015 (m^2/ha)	11.7	45.4	45.4	57.1	43.0	28.5	35.3	28.5	43.0	38.4	38.4	57.1	57.1
Pinus ponderosa basal area in 1910 (% of total)	100	99.9	99.9	96.3	78.8	97.7	100	97.7	78.8	61.8	61.8	96.3	96.3
Pinus ponderosa basal area in 2015 (% of total)	69.8	81.7	81.7	95.4	37.2	78.6	100	78.6	37.2	27.4	27.4	95.4	95.4

Note. An asterisk (*) denotes inner ring date when pith dates could not be estimated accurately.
The historic fire-return interval for each tree was calculated across years prior to 1910 from all trees sampled for fire frequency within the stand (polygon) the tree was located

TABLE 2 Species-level Pearson product–moment correlations of detrended $\Delta^{13}C$ chronologies versus monthly resolution climate variables for 1950 to 2014

Variable	Jan	Feb	Mar	Apr	May	Jun	Jul	Aug	Sep	Oct	Nov	Dec	Water year	JJA
Precip pp	0.18	**0.42**	0.07	**0.34**	0.10	0.08	**0.33**	*0.29*	0.01	0.02	−0.05	0.11	**0.51**	**0.46**
T_{max} pp	−0.01	−0.13	−0.02	−0.14	−0.05	*−0.28*	−0.20	*−0.41*	−0.09	−0.15	−0.05	−0.02	**−0.34**	**−0.39**
VPD pp	−0.09	−0.11	−0.10	−0.24	−0.10	**−0.37**	**−0.33**	**−0.47**	−0.12	−0.19	−0.03	0.04	**−0.54**	**−0.50**
Cloud pp	0.09	−0.06	−0.06	−0.11	−0.22	0.02	0.24	**0.42**	0.03	0.06	−0.07	−0.17	0.09	**0.43**
CMD pp	-	-	0.04	−0.18	−0.13	−0.25	**−0.31**	**−0.39**	0.05	−0.01	-	-	**−0.57**	**−0.49**
PDSI pp	**0.44**	**0.52**	**0.49**	**0.48**	**0.46**	**0.45**	**0.46**	**0.57**	**0.54**	**0.46**	*0.30*	0.25	**0.57**	**0.53**
Precip gf	0.16	*0.31*	0.09	0.17	0.12	0.12	0.20	**0.45**	−0.16	−0.06	*−0.26*	−0.12	**0.54**	**0.51**
T_{max} gf	0.06	−0.08	−0.05	−0.22	−0.14	**−0.39**	−0.20	**−0.51**	−0.05	−0.02	0.19	0.06	**−0.46**	**−0.45**
VPD gf	0.04	−0.11	−0.08	−0.26	−0.18	**−0.44**	*−0.31*	**−0.51**	−0.03	−0.03	*0.28*	0.18	**−0.58**	**−0.51**
Cloud gf	0.11	0.07	0.03	0.12	−0.11	0.06	0.24	**0.42**	−0.02	0.01	−0.13	−0.22	**0.38**	**0.42**
CMD gf	-	-	0.17	−0.14	−0.16	−0.21	−0.24	**−0.50**	0.21	0.09	-	-	**−0.54**	**−0.52**
PDSI gf	**0.42**	**0.46**	**0.46**	**0.48**	**0.42**	**0.45**	**0.47**	**0.59**	**0.44**	**0.33**	0.13	−0.01	**0.54**	**0.55**

Note. Species are indicated by abbreviations after variable names (pp = ponderosa pine, gf = grand fir). Significance at $p < 0.05$ and $p < 0.01$ is denoted by italics and bold, respectively. Water year was calculated as the previous September through the current August. JJA stands for the June, July, and August mean values. T_{max} is maximum temperature. VPD is vapor pressure deficit. Cloud is the CRU gridded cloud cover % for the nearest 0.5° grid cell. CMD is climatic moisture deficit. PDSI is Palmer Drought Severity Index for Oregon Climate Division 5.

pressure deficit, and water year precipitation (Figure 6). These data strongly identified variables associated with summer evaporative demand to have been more important for trees that experienced increased drought stress over time compared to water year precipitation. The weaker influence of precipitation is not surprising since spatial variation in mean annual precipitation at our site is generally in the range of 70–100 cm (Figure 1b), which is relatively high compared to the 28–76 cm range for most ponderosa pine forests, but not as high as the west face of the Sierra Nevada Mountains where ponderosa pine often occurs at elevations where annual precipitation regularly exceeds 100 cm (Burns & Honkala, 1990). The two trees that most strongly drive the relationships between change in $\Delta^{13}C$ and the correlations between $\Delta^{13}C$ and either of VPD or T_{max} (trees 10 and 11 from Table 1) were not unique in any feature and located in different stands. Therefore, the relationships from Figure 6 should be relatively robust and would presumably display similar trends if

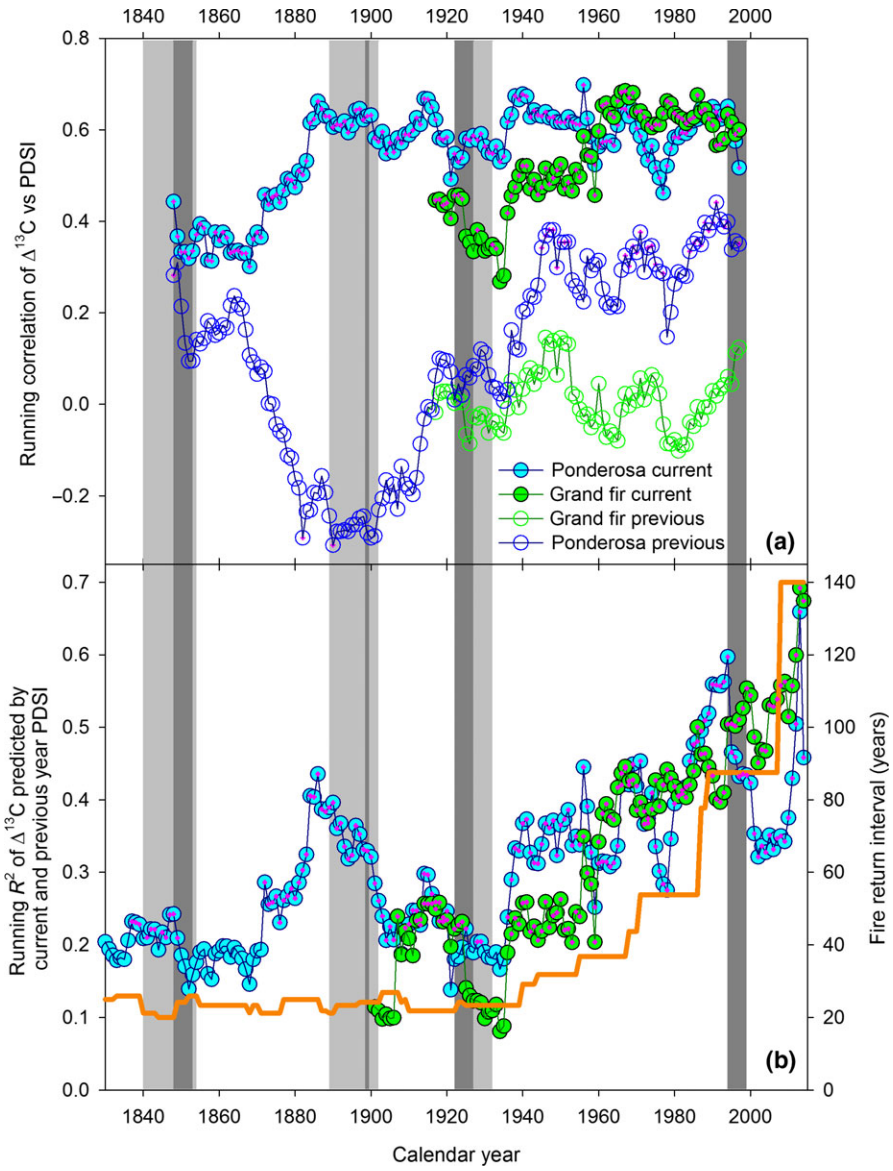

FIGURE 3 The stability of the $\Delta^{13}C$ versus current and previous year Palmer Drought Severity Index (PDSI) is indicated by 35-year moving correlations (a), or coefficients of determination (b). In (b), we also plotted 100-year moving fire frequency data for comparison. Pink crosses within moving correlation data points indicate significance at $p < 0.05$ for the period in question. All values are plotted for the midpoint year of the 35-year moving window. In (a), any values lacking a 35-year window were omitted whereas in (b) the values are plotted for all years, but for the earliest 18 years and latest 17 years the moving window shrinks toward representing only the later or earlier half of the 35-year period, respectively. Light gray bars represent periods of pandora moth outbreaks and defoliation of ponderosa pine at the Pringle Falls locations near the study area (sensu Speer et al., 2001), whereas dark gray bars represent years with growth suppression of the ponderosa pine trees at our study site that likely correspond to the years of greatest local pandora moth defoliation [Colour figure can be viewed at wileyonlinelibrary.com]

additional trees were to have been sampled. Altogether, for our study site, summer evaporative conditions in combination with increased stand density have driven increased drought stress for a given drought severity (e.g., Figure 3b) in the >100 years since fire has been excluded from this landscape.

A recent, global meta-analysis of leaf gas exchange predicts how woody plants respond to changes in $[CO_2]$ (Voelker et al., 2016). We used these predictions, in combination with carbon stable isotope theory and photosynthetic assimilation rate (A) versus leaf internal $[CO_2]$ (c_i) curves from ponderosa pine from this region, in order to estimate how much assimilation and stomatal conductance have changed over time (see Methods). Although A has climbed steadily over time due to rising $[CO_2]$, increasing drought stress has resulted in A being lower than predicted over time by as much as 10% recently (Figure 7a,b). Data from across many plant species show that stomatal conductance (g_s) decreases in response to rapid increases in $[CO_2]$ (Engineer et al., 2016). However, the trends from Voelker et al. (2016) predict long-term increases in $[CO_2]$ should result in progressively greater g_s to accommodate such a large rise in reconstructed values of A. Data from this study indicate that the trajectory of g_s displayed no long-term trend (Figure 7c). Consequently, g_s has been increasingly lower than predicted by up to about 20% compared to that predicted (Figure 7d) and corresponding to increasing drought stress (Figure 3a,b).

4 | DISCUSSION

The evidence gathered here including tree-ring fire histories, forest inventory and tree-ring $\Delta^{13}C$, collectively demonstrate how fire deficits have increased stand basal area leading to increased occupancy of these dry sites and drought stress. Overall, both old ponderosa pine and younger grand fir trees displayed increasing sensitivity of leaf gas exchange (i.e., $\Delta^{13}C$) to PDSI and this closely matched the trajectory of fire-return interval (Figure 3b). In ponderosa pine, this

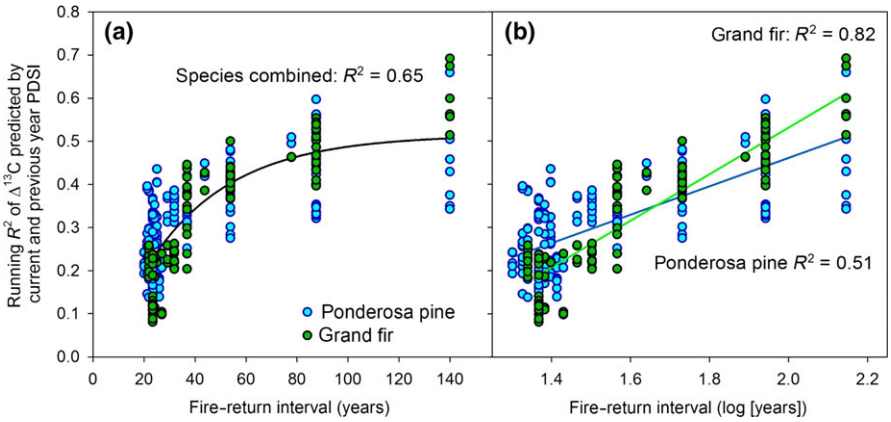

FIGURE 4 35-year moving coefficients of determination (R^2) for Δ^{13}C predicted by current and previous year Palmer Drought Severity Index (PDSI) plotted versus the among-stand average 100-year moving fire-return interval (FRI) across ponderosa pine and grand fir combined (a) and across each species separately after log-transformation of fire-return intervals (b). Each data point represents one year for either species [Colour figure can be viewed at wileyonlinelibrary.com]

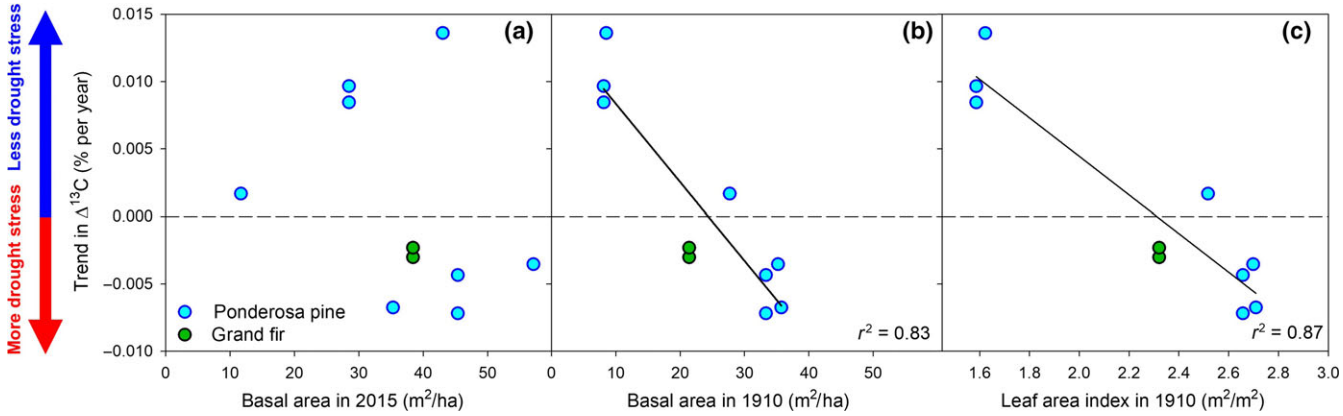

FIGURE 5 Temporal trends of individual trees Δ^{13}C since 1860 versus basal area of the stand where that tree was measured in 2015 (a), versus back-predicted basal area for 1910 (b), and versus back-predicted leaf area index in 1910 (c). 1910 is the year the last fire occurred in most stands we studied. The lowest 2015 basal area is due to logging of most large ponderosa pine trees in that stand during the early 1990s. Without logging, this stand is predicted to have had basal area of about 29 m^2/ha, which would not change the lack of a relationship between Δ^{13}C trend versus basal area in 2015. Only the two oldest grand fir sampled were included because they had tree-ring data that extended to within 15 years of 1860. Blue and red vertical arrows aligned next to the y-axis indicate the direction of increasing or decreasing drought stress based on temporal trend in Δ^{13}C [Colour figure can be viewed at wileyonlinelibrary.com]

increasing drought sensitivity was associated with an increasing influence of current and previous year PDSI, whereas in grand fir, only the influence of current year PDSI increased (Figure 3a). Among the long-term trends in increasing sensitivity to PDSI for ponderosa pine is a pronounced trough from *ca*.1895 to 1935 (Figure 3b), which was driven in part by a decline in the influence of previous year PDSI (Figure 3a). This apparently anomalous pattern appears to be driven in part by one or more defoliation events of ponderosa pine in this region. Speer et al. (2001) found that pandora moth outbreaks were responsible for large defoliation events near our study area occurring ca. 1840–1854, 1889–1902, and 1923–1932 whereas at our site we inferred a modern defoliation from 1994–1999 and three historical defoliation events across a narrower but overlapping set of years compared to the regional patterns (i.e., 1848–1854, 1899, and 1922–25; Figure 3a,b). The amount of variation in Δ^{13}C explained by PDSI tended to be lower in years when inferred defoliation events occurred and for 5–10 years thereafter (Figure 3b). The 1899 growth suppression event at our site resulted in the most severe single-year growth suppression outside of the more recent 1994–1999 defoliation (*data not shown*). Therefore, the inferred 1899 defoliation may have been severe enough to kill or at least severely impair many ponderosa pine trees at our site and thereby had an outsized influence on stand competition for water many years after. Hence, the "trough" in explained variance from *ca*. 1895 to 1935 (Figure 3b) can largely be explained by the severe 1899 defoliation event in combination with the less severe, but longer defoliation event from 1922 to 1925. Post hoc testing confirms these visual patterns. Data in Figure 3b revealed that compared to R^2 values from 10 years previous to defoliation events, R^2 values were lower by 0.049 (p = 0.010) during inferred defoliation years. R^2 values were yet lower by 0.081 (p = 0.019) when inferred defoliation years were combined with the five subsequent years after the defoliation ended or lower by 0.095 (p = 0.029) when inferred defoliation years were combined with ten subsequent years after a defoliation ended. Overall, these values corresponded to a 23% reduction in sensitivity of Δ^{13}C to PDSI due to defoliation. Hence, defoliation of ponderosa pines temporarily ameliorated sensitivity of leaf gas exchange to PDSI via declines in stand-level leaf area and reduced

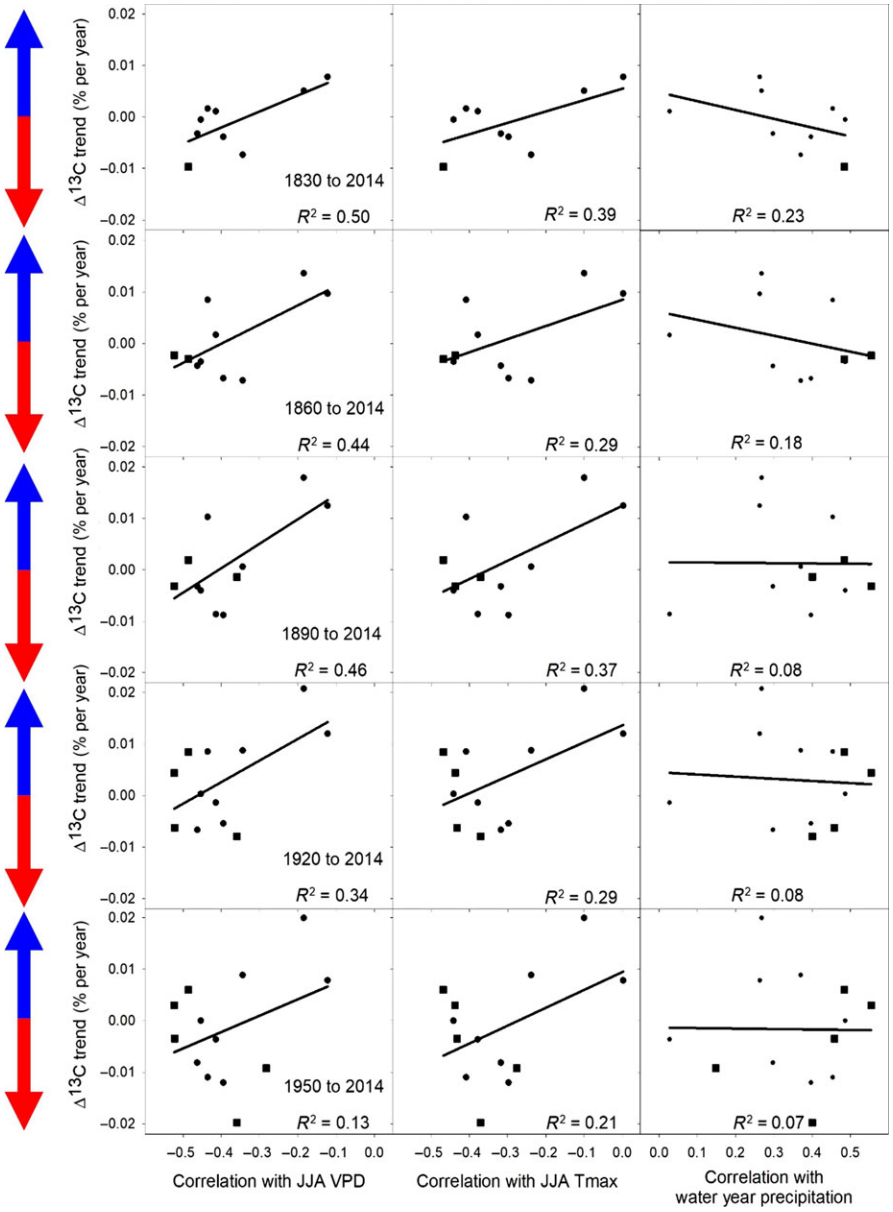

FIGURE 6 Trends in $\Delta^{13}C$ for individual trees across five overlapping time scales plotted versus the 1950–2014 correlation between detrended $\Delta^{13}C$ and mean June–August maximum temperature (T_{max}) or vapor pressure deficit (VPD). Ponderosa pines (circles) were old enough that data extend back to 1830 for each tree but grand fir (squares) are plotted only when tree-ring data extended to within 15 years of the earliest date considered for that panel. As in Figure 5, blue and red vertical arrows aligned next to the y-axis indicate the direction of increasing or decreasing drought stress based on temporal trend in $\Delta^{13}C$ [Colour figure can be viewed at wileyonlinelibrary.com]

demand for water associated with defoliation and mortality of some trees thereafter. These patterns demonstrate that competition for water was partially reversible via defoliation for more than a decade, but that the greater momentum of successional trends after fire suppression has caused competition for water to increase inexorably over the long-term.

At our study area, the increased sensitivity of tree-ring $\Delta^{13}C$ to PDSI across the past >100 years implies that progressively greater competition for water in the absence of disturbances will cause drought stress to continue to increase even if the severity of meteorological drought were not to change. Although we expect this relationship may be generalizable across many forests with increased stand occupancy, this may not be true for all stands in this region or elsewhere because there must be some upper limit for the amount of variation in $\Delta^{13}C$ that can be explained by PDSI. Indeed, in extremely crowded stands of ponderosa pine interannual variability in tree-ring stable isotope signals was found to be lower compared to the same stands after forest thinning treatments (sensu Sohn et al., 2014). Therefore, although our data clearly identify increasing drought stress for a given severity of meteorological drought, it is not yet known whether a critical threshold has been crossed whereby the strength of $\Delta^{13}C$ versus PDSI relationship may underestimate the relative change in drought stress for a given severity of meteorological drought.

Here, we have argued that the increasing dependence of $\Delta^{13}C$ on PDSI in association with prolonged fire deficits and greater stand occupancy is symptomatic of the forests we studied having reduced resistance to drought stress. These symptoms would be expected to result from how strongly isohydric species in high-occupancy stands undergo intense competition for water, but avoid severe drought stress through the strict regulation of stomatal conductance to avoid low xylem water potentials (e.g., Tardieu & Simonneau, 1998; Klein,

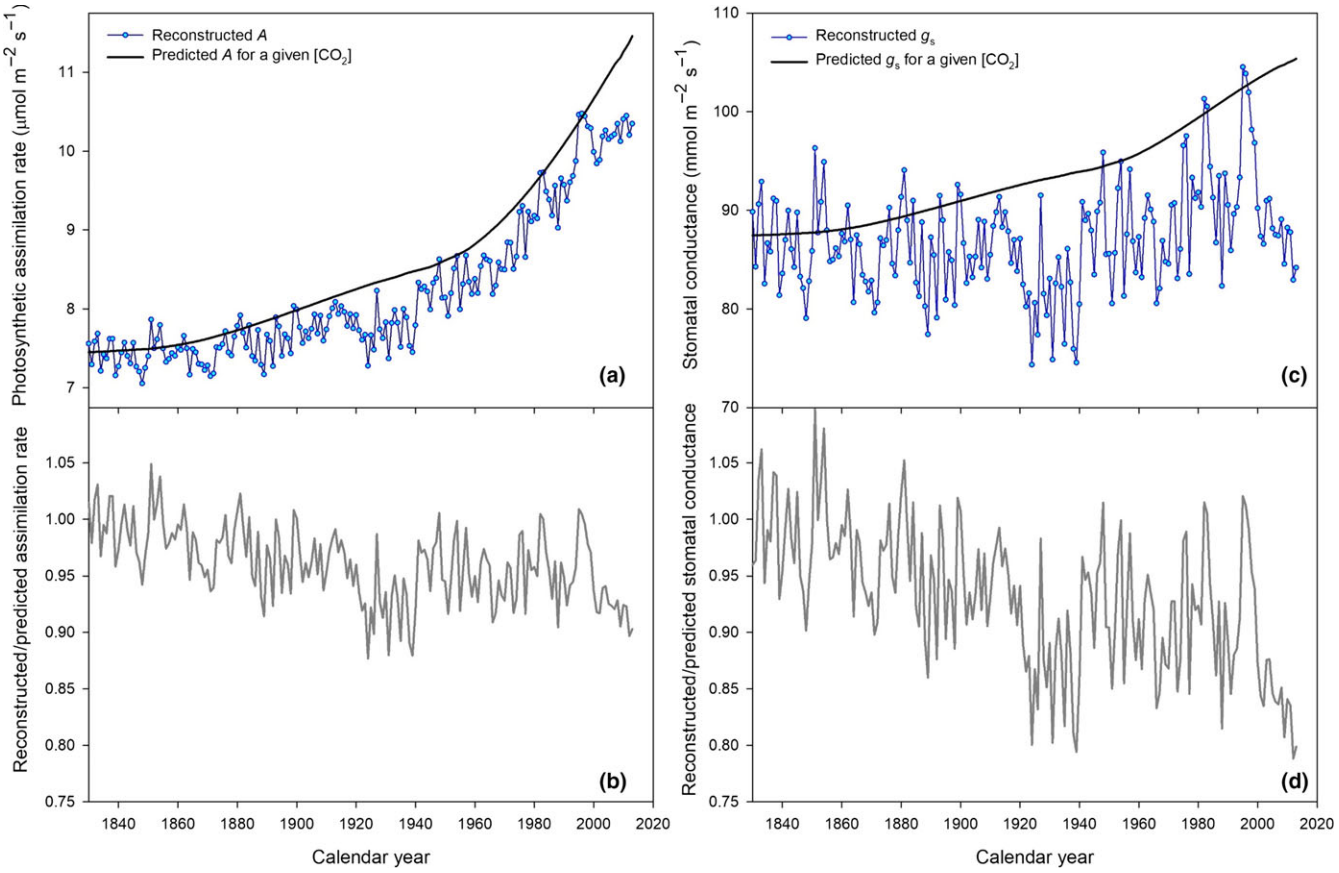

FIGURE 7 Leaf gas exchange patterns reconstructed from $\Delta^{13}C$ and photosynthetic assimilation rate response curves to leaf internal [CO_2] curves (i.e., A-c_i curves, see Methods) for ponderosa pines from 1830 to 2014 compared to that predicted by Voelker et al (2016). Reconstructed and predicted A (a), as well as the ratio of reconstructed to predicted A (b), is shown in the left panels. Reconstructed and predicted stomatal conductance (g_s) (c), as well as the ratio of reconstructed to predicted g_s (d), is shown in the right panels [Colour figure can be viewed at wileyonlinelibrary.com]

2014; Meinzer et al., 2016; Voelker et al., 2018). Hence, forest stands with low stand occupancy and associated lower competition for water are more resistant to drought by avoiding severe stress. Stands experiencing greater drought stress for a given severity of meteorological drought conditions, if they are abundant enough across the landscape, may also result in eroded resilience (Johnstone et al., 2016). Examples of reduced resilience during and after drought include regional tree die-offs in association with beetle outbreaks in the Southwest (Breshears et al., 2005) and California (Fettig et al., 2019; Moore et al., 2017; Young et al., 2017) and increased mortality rates of drought-stressed trees following wildfire (van Mantgem et al., 2013).

Ponderosa pine has a deep rooting habit with substantial uptake of deep soil water, which contrasts with the intermediate to relatively shallow rooting habit in grand fir (Burns & Honkala, 1990; Kerhoulas, Kolb, & Koch, 2013). Although drought stress for a given severity of meteorological drought has increased in both ponderosa pine and grand fir (Figure 3b), based in part on the stand occupancy and leaf area when fire suppression started (Figures 5b5–7c), the trajectory of this increase in drought stress has been greater for the more shallow-rooted grand firs compared to deeply rooted ponderosa pines (Figure 4b). Evaporative conditions, rather than water supply, appear to be the primary meteorological driver of interannual variation in $\Delta^{13}C$ in trees where $\Delta^{13}C$ has decreased over time (Figure 6), which in combination with our other data (Figures 3–5) links meteorological conditions to how drought stress interacted with stand occupancy. These observations suggest grand fir and other small understory trees have been increasingly drying out upper soil horizons during the growing season. In turn, increasing competition at shallow soil depths has forced ponderosa pines to explore deeper rooting zones where winter precipitation recharge from previous years would have a greater influence on soil moisture content (Kerhoulas et al., 2013). It is likely that the capacity of ponderosa pine to accommodate increasingly dry conditions by extracting proportionally more water from deep soil layers has postponed major forest health issues for this species across much of the Pacific Northwest compared to more shallowly rooted grand fir and white fir forests that have higher rates of density dependent and insect or pathogen related mortality (Reilly & Spies, 2016). Massive outbreaks of bark beetles that successfully attack stressed trees have recently killed ponderosa pines across central and southern California (Fettig et al., 2019; Moore et al., 2017). Despite a deep rooting ability in ponderosa pine, droughts will continue to occur and weaken trees and eventually lead to the development of such a beetle outbreak across

this landscape in Oregon. However, ponderosa pine trees incurring less drought stress for a given set of meteorological conditions should have greater defenses against attacks during such outbreaks (Anderegg et al., 2015; Waring & Pitman, 1985).

In accordance with the diversity of forest structures historically present across dry mixed-conifer forests of this region (Merschel et al., 2018), sensitivity of leaf gas exchange to drought stress has not increased ubiquitously across all stands within our study area. Rather, detectable increases in drought stress have tended to occur in stands with ≥25 m^2/ha of basal area when fire suppression started ca. 1910 (Figure 4). The strong influence of stand conditions prior to fire suppression is not a surprising contingency, as other studies in dry mixed-conifer forests have noted that mortality rates by bark beetles (presumably in drought-stressed trees) were linearly related to stand basal area with the predicted basal area for zero mortality occurring between about 12 and 23 m^2/ha (Fettig, Borys, & Dabney, 2010; Hayes, Fettig, & Merrill, 2009). Interestingly, there also seems to be an inflection point between 10 and 35 m^2/ha that corresponds to when surface fires affecting mixed-conifer forest canopies become much more likely to torch and kill the stand (Safford et al., 2009; Stephens et al., 2018). The general rule we propose, for how competition and drought stress is related to stand basal area, would certainly be modified by the presence of shallow, rocky, or nutrient-poor soils. There is also likely to be important variation in what level of basal area induces drought stress depending on species composition that our data set cannot fully address. However, for most dry mixed-conifer forests, stands with basal area ≤25 m^2/ha appear to be more able to resist prolonged drought conditions because lower competition for water in these stands helps trees avoid extreme negative water potentials that can cause serious injury, a loss of hydraulic conductance, susceptibility to pests, and tree death (Anderegg et al., 2015).

The effects of $[CO_2]$ on stomatal control of canopy integrated leaf gas exchange are well documented in many studies, but arguably the most robust data set assembled (Voelker et al., 2016) does not specifically address interactions of $[CO_2]$ and drought stress. Previous research using low-frequency signals in tree-ring growth and carbon isotopes in ponderosa pine from the Northern Rocky Mountains found increasing growth rates and iWUE were attributed to increases in $[CO_2]$ (Knapp & Soulé, 2011; Soulé & Knapp, 2015). Trees growing in relatively open environments were selected for these studies to avoid the influence of changes in competition over time. Hence, these studies also cannot address the more common condition in dry mixed-conifer forests of increasing stand occupancy that likely alters recent leaf gas exchange responses to increasing $[CO_2]$. In contrast, our data indicate that trends in leaf gas exchange over the past 105 years depended in part on the trajectory of competition for water, as indicated by $\Delta^{13}C$ having progressively declined where stand basal area exceeded a threshold of 25 m^2/ha or LAI exceeded 2.3 m^2/m^2 in 1910 (Figure 4b,c). To detail how ponderosa pines have responded to increasing $[CO_2]$ and fire exclusion, we calculated interannual variability in A and g_s of ponderosa pines and compared these to the trends expected from a global meta-analysis of leaf gas exchange responses to $[CO_2]$ (Voelker et al., 2016). These results indicated that A and g_s of ponderosa pines only reached the global $[CO_2]$-response predictions of Voelker et al. (2016) during relatively wet years over recent decades (Figure 7a–b). Although $[CO_2]$-response predictions (i.e., Voelker et al., 2016) indicate g_s would increase with rising $[CO_2]$, and in the absence of drought, even the lack of a long-term trend in reconstructed g_s is somewhat surprising given the apparent increases in drought stress across most stands in our study area. One caveat to the results noted above is that the long-term trends in A and g_s of ponderosa pine are based on an assumption that the A - c_i curves generated recently did not differ with tree age or through time. Since all ponderosa pines were quite old (Table 1) and would have nearly reached their asymptotic height, age is unlikely to have impacted trends in $\Delta^{13}C$, A or g_s through changes in hydrostatic tensions on the xylem stream that can modulate stomatal behavior. Summer precipitation shows no significant trend in this region but average daily temperatures have been increasing, driven primarily by daily minimum temperatures being nearly 3°C greater over recent years compared to 1895 (*data not shown*). On the one hand, this warming trend could have caused A to have been lower during earlier decades than predicted by the temperature-invariant A - c_i curves, due to the positive relationship between temperature and mesophyll conductance (Flexas, Ribas-Carbó, Diaz-Espejo, Galmés, & Medrano, 2008). On the other hand, if these forests are becoming more drought-stressed in mid- to late summer due to greater competition, this would tend to cause these forests to shift the peak in gross primary production to earlier in the growing season when cooler temperatures prevail and thereby counteract the influence of warming minimum temperatures on mesophyll conductance and A over time. Finally, it is possible that increasing $[CO_2]$ could have modified A - c_i curves, most likely through reduced leaf nitrogen content in ponderosa pine (sensu Becklin, Medeiros, Sale, & Ward, 2014) and/or changes in other leaf properties that could increase the resistance to diffusion of CO_2 from stomatal chambers to chloroplasts. Alternatively, more crowded stands could cause a greater proportion of A to be conducted by needles in the lower canopy that tend to have lower A for a given c_i (Crouse & Ellsworth, 2004). For both of these last two scenarios, the reconstructed A and g_s could be biased toward what would otherwise have been stronger drought-induced declines in A and g_s over time in absolute terms and compared to that predicted by Voelker et al. (2016).

The combination of greater stand occupancy and associated leaf area, with estimates of a quasi-stable g_s over the past 100 years, suggests stand-level transpiration rates have increased, despite all other evidence suggesting drought stress has also increased. The warming trends in minimum temperatures noted above would have tended to drive greater evapotranspiration when soil moisture permits over recent decades. Therefore, increases in stand-level (evapo)-transpiration must have resulted in some combination of greater soil drying during the summer as well as increased water extraction from lower soil depths or utilization of groundwater. Since shallow-rooted grand fir and other small understory and mid-story trees have

apparently already been utilizing more of the soil water in upper soil horizons, this likely indicates that old ponderosa pines are increasingly utilizing deeper soil water or ground water. Hence, the steady stomatal conductance in these old-growth ponderosa pines likely reflects their exploiting increasing [CO_2] during wet years and allocating this extra carbon toward deeper soil exploration during dry years. However, the benefits of extra carbon for root exploration may eventually become too costly for the hydraulic system, depending on the total soil depth, resistance of the soil to deeper root exploration, hydraulic resistance from an increasing pathlength and the depth of the water table.

Fire deficits have caused greater stand density and basal area across mixed-conifer forests of the Western United States—resulting in many montane landscapes being less resistant and resilient to widespread mortality events associated with drought stress, bark beetles, and wildfire. Although the landscape we sampled has so far avoided such catastrophic consequences, long-term patterns in $\Delta^{13}C$ demonstrate that drought stress for a given drought severity has increased for old ponderosa pines and younger grand firs. At the stand scale, the magnitude of these effects was associated with stand basal area in 1910, a year that generally marks the start of widespread fire suppression efforts (Pyne, 1982). Hence, increasing drought stress has occurred due to a lack of fires, and the establishment and in-growth of small ponderosa pine and grand fir. For old ponderosa pines, since the 1800s, A has increased while g_s has shown no long-term trend. These reconstructions of leaf gas exchange rates did not keep pace with global predictions except in very wet years, indicating that the effects of increasing [CO_2] are essentially as predicted in the absence of increases in drought stress associated with fire deficits and increased stand occupancy. Across the Western United States, heat and drought severity are increasing and snowpack is decreasing (IPCC, 2013; Mote, Li, Lettenmaier, Xiao, & Engel, 2018) which will make relatively wet years, when trees can take advantage of higher [CO_2], less frequent. Moreover, longer and drier growing seasons would be expected for denser forests in the Pacific Northwest, where canopy cover tends to promote lower snowpack and earlier snowmelt (Dickerson-Lange et al., 2017). Therefore, without a landscape scale approach to judicious management of more wildfires for ecological benefits as well as greater investments in management that combines thinning and prescribed fire to maintain lower maintain lower tree densities (sensu Bradford & Bell, 2017), old mixed-conifer forests like those we sampled in Central Oregon will increasingly cross a threshold that makes them less resistant to drought and less resilient to bark beetle outbreaks and wildfire.

ACKNOWLEDGEMENTS

We thank Chris Ratcliff and Sierra Oxborrow for their careful processing of tree-rings for stable isotope analyses. We also thank two anonymous reviewers whose insightful comments improved this manuscript. This research was supported by joint venture agreement 14-JV-1126191952-095 between the USDA Forest Service and Oregon State University. SLV was also supported by the Utah Agricultural Experiment Station project UTA01304.

ORCID

Steven L. Voelker https://orcid.org/0000-0002-0110-3381
Frederick C. Meinzer https://orcid.org/0000-0003-2387-2031

REFERENCES

Anderegg, W. R. L., Hicke, J. A., Fisher, R. A., Allen, C. D., Aukema, J., Bentz, B., … Zeppel, M. (2015). Tree mortality from drought, insects, and their interactions in a changing climate. *New Phytologist*, *208*, 674–683. https://doi.org/10.1111/nph.13477

Applequist, M. P. (1958). A simple pith locator for use with off-center increment cores. *Journal of Forestry*, *56*, 141.

Arno, S. F., & Sneck, K. M. (1977). *A method for determining fire history in coniferous forests of the mountain west*. U.S. Forest Service General Technical Report, GTR-INT-42.

Becklin, K. M., Medeiros, J. S., Sale, K. R., & Ward, J. K. (2014). Evolutionary history underlies plant physiological responses to global change since the last glacial maximum. *Ecology Letters*, *17*, 691–699. https://doi.org/10.1111/ele.12271

Bekker, M. F., & Taylor, A. H. (2001). Gradient analysis of fire regimes in montane forests of the southern Cascade Range, Thousand Lakes Wilderness, California, USA. *Plant Ecology*, *155*, 15–28.

Bottero, A., D'Amato, A. W., Palik, B. J., Bradford, J. B., Fraver, S., Battaglia, M. A., & Ahserin, L. A. (2017). Density-dependent vulnerability of forest ecosystems to drought. *Journal of Applied Ecology*, *54*, 1605–1614. https://doi.org/10.1111/1365-2664.12847

Bradford, J. B., & Bell, D. M. (2017). A window of opportunity for climate-change adaptation: Easing tree morality by reducing forest basal area. *Frontiers in Ecology and the Environment*, *15*, 11–17.

Breshears, D. D., Cobb, N. S., Rich, P. M., Price, K. P., Allen, C. D., Balice, R. G., … Meyer, C. W. (2005). Regional vegetation die-off in response to global-change-type drought. *Proceedings of the National Academy of Sciences USA*, *102*, 15144–15148. https://doi.org/10.1073/pnas.0505734102

Burns, R. M., & Honkala, B. H. (1990). *Silvics of North America: 1. Conifers. USDA Forest Service Agriculture Handbook 654*, vol *1* (p. 675). Washington, DC: USDA Forest Service.

Cook, E. R., & Krusic, P. J. (2014). *ARSTAN version 44h3: A Tree-ring standardization program based on detrending and autoregressive time series modeling, with interactive graphics*. Palisades, New York, NY: Tree-Ring Laboratory, Lamont-Doherty Earth Observatory of Columbia University.

Cook, E. R., Seager, R., Heim, R. R. Jr, Vose, R. S., Herweijer, C., & Woodhouse, C. (2010). Megadroughts in North America: Placing IPCC projections of hydroclimatic change in a long-term palaeoclimate context. *Journal of Quaternary Science*, *25*, 48–61.

Covington, W. W., & Moore, M. M. (1994). Southwestern ponderosa forest structure: Changes since Euro-American settlement. *Journal of Forestry*, *92*, 39–47.

Crouse, K. Y., & Ellsworth, D. S. (2004). Canopy position affects photosynthetic adjustments to long-term elevated CO_2 concentration (FACE) in aging needles in a mature *Pinus taeda* forest. *Tree Physiology*, *24*, 961–970. https://doi.org/10.1093/treephys/24.9.961

Dickerson-Lange, S. E., Gersonde, R. F., Hubbart, J. A., Link, T. E., Nolin, A. W., Perry, G. H., … Lundquist, J. D. (2017). Snow disappearance timing is dominated by forest effects on snow accumulation in warm winter climates of the Pacific Northwest, United States. *Hydrological Processes*, *31*, 1846–1862. https://doi.org/10.1002/hyp.11144

Dore, S., Montes-Helu, M., Hart, S. C., Hungate, B. A., Koch, G. W., Moon, J. B., … Kolb, T. E. (2012). Recovery of ponderosa pine ecosystem carbon and water fluxes from thinning and stand-replacing fire. *Global Change Biology*, *18*, 3171–3185. https://doi.org/10.1111/j.1365-2486.2012.02775.x

Ehleringer, J. R. (1993). Carbon and water relations in desert plants: An isotopic perspective. In J. R. Ehleringer, A. E. Hall, & G. D. Farquhar (Eds.), *Stable isotopes and plant carbon/water relations* (p. 555). San Diego, CA: Academic Press.

Engineer, C. B., Hashimoto-Sugimoto, M., Negi, J., Israelsson-Nordström, M., Azoulay-Shemer, T., Rappel, W. J., … Schroeder, J. I. (2016). CO_2 sensing and CO_2 regulation of stomatal conductance: Advances and open questions. *Trends in Plant Science*, *21*, 16–30. https://doi.org/10.1016/j.tplants.2015.08.014

Farquhar, G. D., Ehleringer, J. R., & Hubick, K. T. (1989). Carbon isotope discrimination and photosynthesis. *Annual Review of Plant Biology*, *40*, 503–537.

Feng, X. (1998). Long-term c_i/c_a response of trees in western North America to atmospheric CO_2 concentration derived from carbon isotope chronologies. *Oecologia*, *117*, 19–25.

Fettig, C., Borys, R., & Dabney, C. (2010). Effects of fire and fire surrogate treatments on bark beetle-caused tree mortality in the Southern Cascades, California. *Forest Science*, *56*, 60–73.

Fettig, C. J., Klepzig, K. D., Billings, R. F., Munson, A. S., Nebeker, T. E., Negron, J. F., & Nowak, J. T. (2007). Effectiveness of vegetation management practices for prevention and control of bark beetle infestations in coniferous forests of the Western and Southern United States. *Forest Ecology and Management*, *238*, 24–53.

Fettig, C. J., Mortenson, L. A., Bulaon, B. M., & Foulk, P. B. (2019). Tree mortality following drought in the central and southern Sierra Nevada, California, U.S. *Forest Ecology and Management*, *432*, 164–178. https://doi.org/10.1016/j.foreco.2018.09.006

Flexas, J., Ribas-Carbó, M., Diaz-Espejo, A., Galmés, J., & Medrano, H. (2008). Mesophyll conductance to CO_2: Current knowledge and future prospects. *Plant, Cell & Environment*, *31*, 602–621.

Giuggiola, A., Ogée, J., Rigling, A., Gessler, A., Bugmann, H., & Treydte, K. (2016). Improvement of water and light after thinning at a xeric site: Which matters more? A dual isotope approach. *New Phytologist*, *210*, 108–121.

Hagmann, K. R., Franklin, J. F., & Johnson, K. N. (2013). Historical structure and composition of ponderosa pine and mixed-conifer forests in south-central Oregon. *Forest Ecology and Management*, *304*, 492–504. https://doi.org/10.1016/j.foreco.2013.04.005

Hagmann, K. R., Franklin, J. F., & Johnson, K. N. (2014). Historical conditions in mixed-conifer forests on the eastern slopes of the northern Oregon Cascade Range, USA. *Forest Ecology and Management*, *330*, 158–170. https://doi.org/10.1016/j.foreco.2014.06.044

Hayes, C. J., Fettig, C. J., & Merrill, L. D. (2009). Evaluation of multiple funnel traps and stand characteristics for estimating western pine beetle-caused tree mortality. *Economic Entomology*, *106*, 2170–2182. https://doi.org/10.1603/029.102.0621

Hessburg, P. F., Spies, T. A., Perry, D. A., Skinner, C. N., Taylor, A. H., Brown, P. M., … Riegel, G. (2016). Tamm review: Management of mixed-severity fire regime forests in Oregon, Washington, and Northern California. *Forest Ecology and Management*, *366*, 221–250. https://doi.org/10.1016/j.foreco.2016.01.034

Holmes, R. L. (1983). Program COFECHA User's Manual. *Laboratory of Tree-Ring Research*. The University of Arizona, Tucson, USA.

Hood, S. M., Baker, S., & Sala, A. (2016). Fortifying the forest: Thinning and burning increase resistance to a bark beetle outbreak and promote forest resilience. *Ecological Applications*, *26*, 1984–2000. https://doi.org/10.1002/eap.1363

Hood, S. M., Sala, A., Heyerdahl, E. K. J., & Boutin, M. (2015). Low-severity fire increases tree defense against bark beetle attacks. *Ecology*, *9*, 1846–1855. https://doi.org/10.1890/14-0487.1

IPCC (2013). *Climate change 2013: The physical science basis*. Contribution of Working Group I to the Fifth Assessment Report of the Intergovernmental Panel on Climate Change [Stocker, T., Qin D, Plattner G-K, et al., (Eds.)]. Cambridge University Press, Cambridge, United Kingdom and New York, NY, USA, 1535 pp. https://doi.org/10.1017/CBO9781107415324

Johnston, J. D. (2017). Forest succession along a productivity gradient following fire exclusion. *Forest Ecology and Management*, *392*, 45–57. https://doi.org/10.1016/j.foreco.2017.02.050

Johnstone, J. F., Allen, C. D., Franklin, J. F., Frelich, L. E., Harvey, B. J., Higuera, P. E., … Turner, M. G. (2016). Changing disturbance regimes, ecological memory, and forest resilience. *Frontiers in Ecology and the Environment*, *14*, 369–378. https://doi.org/10.1002/fee.1311

Jump, A. S., Ruiz-Benito, P., Greenwood, S., Allen, C. D., Kitzberger, T., Fensham, R., … Lloret, F. (2017). Structural overshoot of tree growth with climate variability and the global spectrum of drought-induced forest dieback. *Global Change Biology*, *23*, 3742–3757. https://doi.org/10.1111/gcb.13636

Kalies, E. L., & Yocom Kent, L. L. (2016). Tamm review: Are fuel treatments effective at achieving ecological and societal objectives? A systematic review. *Forest Ecology and Management*, *375*, 84–95.

Kerhoulas, L. P., Kolb, T. E., & Koch, G. W. (2013). Tree size, stand density, and the source of water used across seasons by ponderosa pine in northern Arizona. *Forest Ecology and Management*, *289*, 425–433. https://doi.org/10.1016/j.foreco.2012.10.036

Klein, T. (2014). The variability of stomatal sensitivity to leaf water potential across tree species indicates a continuum between isohydric and anisohydric behaviours. *Functional Ecology*, *28*, 1313–1320. https://doi.org/10.1111/1365-2435.12289

Knapp, P. A., & Soulé, P. T. (2011). Increasing water-use efficiency and age-specific growth responses of old-growth ponderosa pine trees in the Northern Rockies. *Global Change Biology*, *17*, 631–641.

Knapp, P. A., Soulé, P. T., & Maxwell, J. T. (2013). Mountain pine beetle selectivity in old-growth ponderosa pine forests, Montana, USA. *Ecology and Evolution*, *3*, 1141–1148. https://doi.org/10.1002/ece3.522

Law, B. E., Sun, O. J., Campbell, J., Van Tuyl, S., & Thornton, P. E. (2003). Changes in carbon storage and fluxes in a chronosequence of ponderosa pine. *Global Change Biology*, *9*, 510–524.

Leavitt, S. W., & Danzer, S. R. (1993). Methods for batch processing small wood samples to holocellulose for stable-carbon isotope analysis. *Analytical Chemistry*, *65*, 87–89.

Leavitt, S. W., & Long, A. (1988). Stable carbon isotope chronologies of trees from the Southwestern United States. *Global Biogeochemical Cycles*, *2*, 189–198.

Leavitt, S. W., Wright, W. E., & Long, A. (2002). Spatial expression of ENSO, drought, and summer monsoon in seasonal $\delta^{13}C$ of ponderosa pine tree rings in southern Arizona and New Mexico. *Journal of Geophysical Research: Atmospheres*, *107*, ACL3-1–ACL 3-10.

Lloret, F., Keeling, E. G., & Sala, A. (2011). Components of tree resilience: Effects of successive low-growth episodes in old ponderosa pine forests. *Oikos*, *12*, 1909–1920. https://doi.org/10.1111/j.1600-0706.2011.19372.x

Lutz, J. A., van Wagtendonk, J. W., & Franklin, J. F. (2010). Climatic water deficit, tree species ranges, and climate change in Yosemite National Park. *Journal of Biogeography*, *37*, 936–950. https://doi.org/10.1111/j.1365-2699.2009.02268.x

Marshall, J. D., & Monserud, R. A.(1996). Homeostatic gas-exchange parameters inferred from $^{13}C/^{12}C$ in tree rings of conifers. *Oecologia*, *105*, 13–21.

McCarroll, D., & Loader, N. J. (2004). Stable isotopes in tree rings. *Quaternary Science Reviews*, *23*, 771–801. https://doi.org/10.1016/j.quascirev.2003.06.017

McDowell, N. G., Adams, H. D., Bailey, J. D., Hess, M., & Kolb, T. E. (2006). Homeostatic maintenance of ponderosa pine gas exchange in response to stand density changes. *Ecological Applications*, *16*, 1164–

1182. https://doi.org/10.1890/1051-0761(2006)016[1164:HMOPPG]2.0.CO;2

McDowell, N. G., Allen, C. D., & Marshall, L. (2010). Growth, carbon isotope discrimination, and drought-associated mortality across a Pinus ponderosa elevational transect. *Global Change Biology*, *16*, 399–415. https://doi.org/10.1111/j.1365-2486.2009.01994.x

McDowell, N. G., Brooks, J. R., Fitzgerald, S., & Bond, B. J. (2003). Carbon isotope discrimination and growth response of old ponderosa pine trees to stand density reductions. *Plant, Cell and Environment*, *26*, 631–644.

Meinzer, F. C., Woodruff, D. R., Marias, D. E., Smith, D. D., McCulloh, K. A., Howard, A. R., & Magedman, A. L. (2016). Mapping "hydroscapes" along the iso- to anisohydric continuum of stomatal regulation of plant water status. *Ecology Letters*, *19*, 1343–1352. https://doi.org/10.1111/ele.12670.

Merschel, A. G., Heyerdahl, E. K., & Spies, T. A. (2018). Influence of landscape structure, topography, and forest type on spatial variation in historical fire regimes, Central Oregon, USA. *Landscape Ecology*, *33*(7), 1195–1209. https://doi.org/10.1007/s10980-018-0656-6.

Merschel, A. G., Spies, T. A., & Heyerdahl, E. K. (2014). Mixed-conifer forests of central Oregon: Effects of logging and fire exclusion vary with environment. *Ecological Applications*, *24*, 1670–1688. https://doi.org/10.1890/13-1585.1

Moore, J., McAfee, L., Jirka, A., Heath, Z., & Smith, B. (2017) *2016 Aerial Survey Results California*. USDA Forest Service, Pacific Southwest Region R5-PR-034.

Mote, P. W., Li, S., Lettenmaier, D. P., Xiao, M., & Engel, R. (2018). Dramatic decline in snowpack in the western US. *Npj Climate and Atmospheric Science*, *1*, 2. https://doi.org/10.1038/s41612-018-0012-1

Parks, S. A., Miller, C., Parisien, M.-A., Holsinger, L. M., Dobrowski, S. Z., & Abatzoglou, J. (2015). Wildland fire deficit and surplus in the western United States, 1984–2012. *Ecosphere*, *6*, 1–13. https://doi.org/10.1890/ES15-00294.1

Pyne, S. J. (1982). *Fire in America: A cultural history of wildland and rural fire (cycle of fire)*. Seattle, WA: University of Washington Press.

R Development Core Team (2017). *R: A language and environment for statistical computing*. Vienna, Austria: R Foundation for Statistical Computing.

Raffa, K. F., Aukema, B. H., Bentz, B. J., Carroll, A. L., Hicke, J. A., Turner, M. G., & Romme, W. H. (2008). Cross-scale drivers of natural disturbances prone to anthropogenic amplification: The dynamics of bark beetle eruptions. *BioScience*, *58*, 501–517. https://doi.org/10.1641/B580607

Ratcliff, C. J., Voelker, S. L., & Nolin, A. W. (2018). Tree-ring carbon isotope records from the western Oregon Cascade Mountains primarily records summer maximum temperatures. *Tree-Ring Research*, *74*, 185–195.

Reed, C. C., Ballantyne, A. P., Cooper, L. A., & Sala, A. (2018). Limited evidence for CO_2-related growth enhancement in northern Rocky Mountain lodgepole pine populations across climate gradients. *Global Change Biology*, *24*, 3922–3937.

Reilly, M. J., & Spies, T. A. (2016). Disturbance, tree mortality, and implications for contemporary regional forest change in the Pacific Northwest. *Forest Ecology and Management*, *374*, 102–110. https://doi.org/10.1016/j.foreco.2016.05.002

Roden, J. S., & Ehleringer, J. R. (2007). Summer precipitation influences the stable oxygen and carbon isotopic composition of tree-ring cellulose in *Pinus ponderosa*. *Tree Physiology*, *27*, 491–501. https://doi.org/10.1093/treephys/27.4.491

Safford, H. D., Schmidt, D. A., & Carlson, C. H. (2009). Effects of fuel treatments on fire severity in an area of wildland-urban interface, angora Fire Lake Tahoe Basin, California. *Forest Ecology and Management*, *258*, 773–787.

Smith, H. Y., & Arno, S. F. (1999). *Eighty-eight years of change in a managed ponderosa pine forest*. Gen. Tech. Rep. RMRS-GTR-23. Ogden, UT: U.S. Department of Agriculture, Rocky Mountain Research Station. 55 p.

Sohn, J. A., Brooks, J. R., Bauhaus, J., Kohler, M., Kolb, T. E., & McDowell, N. G. (2014). Unthinned slow-growing ponderosa pine (*Pinus ponderosa*) trees contain muted isotopic signals in tree rings as compared to thinned trees. *Trees*, *28*, 1035–1051. https://doi.org/10.1007/s00468-014-1016-z

Sohn, J. A., Saha, S., & Bauhaus, J. (2016). Potential of forest thinning to mitigate drought stress: A meta-analysis. *Forest Ecology and Management*, *380*, 261–273. https://doi.org/10.1016/j.foreco.2016.07.046

Soulé, P. T., & Knapp, P. A. (2015). Analyses of intrinsic water-use efficiency indicate performance differences of ponderosa pine and Douglas-fir in response to CO_2 enrichment. *Journal of Biogeography*, *42*, 144–155.

Speer, J. H., Swetnam, T. W., Wickman, B. E., & Youngblood, A. (2001). Changes in pandora moth outbreak dynamics during the past 622 years. *Ecology*, *82*, 679–697. https://doi.org/10.1890/0012-9658(2001)082[0679:CIPMOD]2.0.CO;2

Spies, T. A., Hessburg, P. F., Skinner, C. N., et al.(2018). Old growth, disturbance, forest succession and management in the area of the Northwest Forest Plan. In T. A. Spies, P. Stine, R. Gravenmeir, J. W. Long, & M. Reilly (Eds.), *Synthesis of science to inform land management within the Northwest Forest Plan area*. Gen. Tech. Rep. PNW-GTR-966. Portland, OR: Department of Agriculture, Forest Service, Pacific Northwest Research Station.

Stephens, S. L. (1998). Evaluation of the effects of silvicultural and fuels treatments on potential fire behaviour in Sierra Nevada mixed-conifer forests. *Forest Ecology and Management*, *105*, 21–35. https://doi.org/10.1016/S0378-1127(97)00293-4

Stephens, S. L., Collins, B. M., Fettig, C. J., Finney, M. A., Hoffman, C. M., Knapp, E. E., … Wayman, R. B. (2018). Drought, tree mortality, and wildfire in forests adapted to frequent fire. *BioScience*, *68*, 77–88. https://doi.org/10.1093/biosci/bix146

Szejner, P., Wright, W. E., Belmecheri, S., Meko, D., Leavitt, S. W., Ehleringer, J. R., & Monson, R. K. (2018). Disentangling seasonal and interannual legacies from inferred patterns of forest water and carbon cycling using tree-ring stable isotopes. *Global Change Biology.*, *24*, 5332–5347. https://doi.org/10.1111/gcb.14395

Szejner, P., Wright, W. E., Babst, F., Belmecheri, S., Trouet, V., Leavitt, S. W., … Monson, R. K. (2016). Latitudinal gradients in tree ring stable carbon and oxygen isotopes reveal differential climate influences of the North American Monsoon System. *Journal of Geophysical Research: Biogeosciences*, *121*, 1978–1991. https://doi.org/10.1002/2016jg003460

Tardieu, F., & Simonneau, T. (1998). Variability among species of stomatal control under fluctuating soil water status and evaporative demand: Modelling isohydric and anisohydric behaviours. *Journal of Experimental Botany*, *49*, 419–432. https://doi.org/10.1093/jxb/49.Special_Issue.419

van Mantgem, P. J., Nesmith, J. C. B., Keifer, M., Knapp, E. E., Flint, A., & Flint, L. (2013). Climatic stress increases forest fire severity across the western United States. *Ecology Letters*, *16*, 1151–1156. https://doi.org/10.1111/ele.12151

Vernon, M. J., Sherriff, R. L., van Mantgem, P., & Kane, J. M. (2018). Thinning, tree growth, and resistance to multi-year drought in a mixed conifer forest of Northern California. *Forest Ecology and Management*, *422*, 190–198. https://doi.org/10.1016/j.foreco.2018.03.043

Voelker, S. L., DeRose, R. J., Bekker, M. F., Sriladda, C., Leksungnoen, N., & Kjelgren, R. K. (2018). Anisohydric water use behavior links growing season evaporative demand to ring-width increment in conifers from summer-dry environments. *Trees*, *32*, 735–749. https://doi.org/10.1007/s00468-018-1668-1

Voelker, S. L., Muzika, R., & Guyette, R. P. (2008). Individual tree and stand level influences on the growth, vigor and decline of red oaks in the Ozarks. *Forest Science*, *54*, 8–20.

Voelker, S. L., Brooks, J. R., Meinzer, F. C., Anderson, R., Bader, M.-K.-F., Battipaglia, G., … Wingate, L. (2016). A dynamic leaf gas exchange strategy is conserved in woody plants under changing ambient CO_2: Evidence from carbon isotope discrimination in paleo and CO_2 enrichment studies. *Global Change Biology*, *22*, 899–902. https://doi.org/10.1111/gcb.13102

Waring, R. H., & Pitman, G. B. (1985). Modifying lodgepole pine stands to change susceptibility to mountain pine beetle. *Ecology*, *66*, 889–897.

Young, D. J. N., Stevens, J. T., Earles, J. M., Moore, J., Ellis, A., Jirka, A. L., & Latimer, A. M. (2017). Long-term climate and competition explain forest mortality patterns under extreme drought. *Ecology Letters*, *20*, 78–86. https://doi.org/10.1111/ele.12711

Zang, C., & Biondi, F. (2015). Treeclim: An R package for the numerical calibration of proxy-climate relationships. *Ecography*, *38*, 431–436. https://doi.org/10.1111/ecog.01335

SUPPORTING INFORMATION

Additional supporting information may be found online in the Supporting Information section at the end of the article.

How to cite this article: Voelker SL, Merschel AG, Meinzer FC, Ulrich DEM, Spies TA, Still CJ. Fire deficits have increased drought sensitivity in dry conifer forests: Fire frequency and tree-ring carbon isotope evidence from Central Oregon. *Glob Change Biol*. 2019;25:1247–1262. https://doi.org/10.1111/gcb.14543